

## MONTE CARLO SIMULATIONS OF HEAVY METAL IONS IN WATER

Sean M. Braet\*, Nick Bigham\*, Jeb S. Kegerreis†

Department of Chemistry and Biochemistry, Shippensburg University, Shippensburg, PA 17257

## Abstract

Monte Carlo simulations were utilized to give structural and thermodynamic insight into aqueous heavy metal ion systems. Van der Waals forces were addressed using a Lennard-Jones 12-6 potential and Coulombic forces were accounted for using Wolf's method as an alternative to Ewald Summation techniques. This novel approach for charged systems allowed for computationally efficient assessment of solvation energies, coordination numbers, and radial distribution functions. It was found that this process was successful in calculating the structural and energetic properties of the  $\text{Pb}^{2+}$  (aq) system, but was less successful when applied to  $\text{Cd}^{2+}$  (aq) and  $\text{Zn}^{2+}$  (aq).

†Corresponding Author: jskegerreis@ship.edu

Keywords: Wolf's Method, Monte Carlo, Aqueous System

## Introduction

Aqueous metal ions have critical biological functions as cofactors for enzymes. For example,  $\text{Zn}^{2+}$  is a cofactor for carbonic anhydrase which plays a critical role in oxygen transport.<sup>1</sup> However, in high concentrations, metal ions can be toxic and become dangerous pollutants.<sup>2</sup> Zinc, cadmium, and lead can all lead to significant health problems such as cancer and organ damage.<sup>2</sup> Evaluating the role of metal cofactors or determining methods for removing water pollutants first requires an in depth understanding of their behaviors in aqueous systems.

Simulations can be utilized to determine key properties of aqueous metal ions such as hydration energy and coordination number. Elucidation of thermodynamic and structural information could be applied to the understanding of biological systems or pollution management. In this study, the hydration of  $\text{Cd}^{2+}$ ,  $\text{Pb}^{2+}$ , and  $\text{Zn}^{2+}$  was analyzed through a classical NVT simulation. Previous studies of these systems have utilized molecular dynamics (MD) techniques.<sup>1,3</sup> While MD simulations are effective, they can also be computationally expensive when dealing with a system containing large numbers of molecules. Monte Carlo integration offers a more computationally efficient method because its computational cost does not increase as rapidly as the number of particles in a system increases.<sup>4</sup> Increased computational efficiency thus opens the possibility of exploring such systems in undergraduate research settings. In this work, the energetics and solvation structure of hydrated metal ion systems were evaluated using a classical Monte Carlo process.

Traditionally, the calculation of interaction potential energies (a necessary step in any classical simulation) becomes a main hurdle with respect to computational efficiency. While a simple function such as a Lennard-Jones 12-6 potential can account for short-ranged Van der Waals interactions, accounting for electrostatic interactions in the form of Coulombic potentials becomes problematic due to their relative long range of influence. The standard method for dealing with long range interactions in systems with charges is called Ewald Summation. However, Ewald Summation requires using replicate systems and rapidly increases computational cost for larger simulations.<sup>5</sup> Wolf's Method, which scales linearly with system size, offers a more computationally ef-

ficient alternative.<sup>5-7</sup> In Wolf's Method, a radial cutoff is applied to the system and a dampening function is introduced.<sup>6</sup> This allows for interactions beyond the cutoff to be accounted for by the dampening of short range interactions.<sup>5-7</sup> While this method has been applied to homogeneous systems<sup>5-9</sup>, very little work has been done applying Wolf's method to heterogeneous systems.<sup>10</sup> In this work, Wolf's method was applied to determine solvation energies and radial distribution functions of  $\text{Zn}^{2+}$ ,  $\text{Cd}^{2+}$ , and  $\text{Pb}^{2+}$  aqueous systems.

## Methodology

All simulations were carried out with an in-house code written in FORTRAN. A temperature of 25 °C was chosen, along with a density of 0.03343 molecules/Å<sup>3</sup> to be able to compare our results with previous work. A rigid SPC/E model was utilized to represent pure water.<sup>11</sup> The SPC/E model represents the atoms of a water molecule as an extended simple point charge.<sup>11</sup> SPC/E parameters are shown in Table 1. The water molecules were allowed to undergo rotations and translations but the bond distances and angles remained fixed to reduce computational time. For each water molecule, 100000 Monte Carlo steps were taken resulting in a standard deviation of approximately 0.01 kcal/mol. The SPC/E model yields results that closely match experimental results without compromising computational efficiency. Metal ions were treated as fixed point charges at the origin with total charges of +2e. All simulations utilized periodic boundary conditions with a box length of 24.64 Å.

For each system studied, a classical simulation was enacted with average potential energies calculated via

$$\langle V \rangle = \frac{\int d\vec{r} V(\vec{r}) e^{-\beta V(\vec{r})}}{\int d\vec{r} e^{-\beta V(\vec{r})}} \quad [1]$$

where  $V(\vec{r})$  is the total interaction potential energy,  $\vec{r}$  represents

Table 1. Table of Simulation and SPC/E Parameters

Simulation Parameters	
Water Molecules	500
$r_c$ (Å)	10.00
$\alpha$ Water (Å <sup>-1</sup> )	0.3200
$\alpha$ Metal (Å <sup>-1</sup> )	0.2200
$q$ Oxygen (e) <sup>11</sup>	-0.8476
$q$ Hydrogen (e) <sup>11</sup>	0.4238
Water O-H Bond Length (Å) <sup>11</sup>	1.000
Water Bond Angle (deg) <sup>11</sup>	109.47

the collection of spatial coordinates of all particles within the system, and  $\beta$  is equal to the inverse of the product of the Boltzmann constant times the temperature in Kelvin. In order to establish a computationally efficient method, a Monte Carlo process was enacted to evaluate [1] by taking the total integrand and splitting it into a sampling function and a Monte Carlo integrand:<sup>4</sup> the sampling function was chosen to be  $e^{-\beta V(\vec{r})}$  (normalized by the integral  $\int d\vec{r} e^{-\beta V(\vec{r})}$  found in the denominator of [1]) and the Monte Carlo integrand was thus  $V(\vec{r})$ . In Monte Carlo integration, the sampling function acts as a probability distribution and thus directs the importance of differing random configurations within a simulation. In our work, a Metropolis random walk was enacted with the choice of sampling function indicated above, and thus configurational changes were accepted or rejected based on the effects of the subsequent total potential energies on the function  $e^{-\beta V(\vec{r})}$ .

The total interaction potential was calculated as a sum of Van der Waals and electrostatic interactions. A Lennard-Jones 12-6 potential (parameters in Table 2) was used to evaluate Van der Waals interactions. The Lennard-Jones 12-6 potential takes the form

$$V_{ij}^{VDW}(r_{ij}) = 4\epsilon_{ij} \left[ \left( \frac{\sigma_{ij}}{r_{ij}} \right)^{12} - \left( \frac{\sigma_{ij}}{r_{ij}} \right)^6 \right], \quad [2]$$

where  $V_{ij}^{VDW}$  represents the Van der Waals interaction potential energy between two atoms,  $\epsilon_{ij}$  and  $\sigma_{ij}$  are related to the potential well minimum and the zero-potential distance, respectively, and  $r_{ij}$  represents the distance between the particles. Particles also interact electrostatically via

$$V_{ij}^{Col}(r_{ij}) = \frac{q_i q_j}{r_{ij}}, \quad [3]$$

where  $V_{ij}^{Col}(r)$  represents the coulombic interaction potential between atoms  $i$  and  $j$ , and  $q$  represents the charge of each particle. An issue arises with the direct use of [3] in molecular simulations as the relatively weak  $1/r$  decay requires a prohibitive number of long-range interactions to be accessed to get an accurate value for potential interactions. In order to calculate said long range interactions while maintaining computational efficiency, other methods are thus required. In this study, Wolf's Method was utilized as an alternative to the more standard Ewald Summation techniques used to address this issue. Wolf's Method approximates the effects of long range interactions by using a cutoff radius and a damped shifted potential function for interactions inside of the cutoff radius.<sup>7</sup> This allows for contributions of long range interactions beyond the cutoff to be estimated by dampening interactions within the cutoff. By utilizing the damp shifted force application of this method,<sup>6</sup> the total interaction potential can be calculated through the use of a single analytical function that sums Van der Waals contributions and the modified electrostatic potential interacts as

**Table 2.** Lennard Jones Parameters for Metal Ion to Oxygen Interactions

Interaction	$\sigma$ (Å)	$\epsilon$ (kcal/mol)
O-O <sup>11</sup>	3.166	0.1500
O-Zn <sup>1</sup>	1.950	0.2500
O-Cd <sup>3</sup>	2.700	0.0060
O-Pb <sup>3</sup>	3.000	0.1912

$$V(r_{ij}) = \frac{1}{2} \sum_{i=1} \sum_{j \neq i} 4\epsilon_{ij} \left[ \left( \frac{\sigma_{ij}}{r_{ij}} \right)^{12} - \left( \frac{\sigma_{ij}}{r_{ij}} \right)^6 \right] + q_i q_j \left[ \frac{\text{erfc}(\alpha r_{ij})}{r_c} - \frac{\text{erfc}(\alpha r_c)}{r_c} + \left( \frac{\text{erfc}(\alpha r_c)}{r_c^2} + \frac{2\alpha e^{(-\alpha^2 r_c^2)}}{\sqrt{\pi} r_c} \right) (r_{ij} - r_c) \right], \quad [4]$$

where  $\alpha$  represents the dampening parameter of the potential function,  $r_c$  represents a chosen cutoff radius, and  $\text{erfc}$  is the complimentary error function. Simulations thus proceed by choosing a  $r_c$ , and then converging the calculation of total average potential energy through optimization of  $\alpha$ .<sup>6-10</sup> It should be noted that [4] represents one version of Wolf's method that neglects self and long range terms.<sup>5,6,8</sup> In previous work by Waibel et al. and Fanourgakis et al, contributions from the self-term

$$V_{self}(r) = \left[ -\frac{\text{erfc}(\alpha r_c)}{2r_c} + \frac{\alpha}{\sqrt{\pi}} + \frac{\alpha e^{(-\alpha^2 r_c^2)}}{\sqrt{\pi}} \right] \sum_{i=1} q_i^2, \quad [5]$$

and long range term

$$V_{long}(r_{ij}) = \frac{1}{2} \sum_i \sum_j \frac{q_i q_j \text{erf}(\alpha r_{ij})}{r_{ij}} \quad [6]$$

were found to be approximately zero for the homogenous systems.<sup>6,8</sup> To keep the functional form of the potential as simple as possible, our simulations did not include contributions [5] and [6], and thus our work acts as grounds to see if such terms play a more critical role in the aqueous metal ion systems of interest; if our results differ greatly from previously established values, the possibility of [5] and [6] being important under our simulation conditions becomes a point of interest.

To determine solvation energies, the potential energy for each aqueous metal ion system was subtracted from the potential energy of water,<sup>12,13</sup>

$$\langle V_{sol} \rangle = \langle V_{ionic} \rangle - \langle V_{water} \rangle \quad [7]$$

as the only difference between the simulations leading to the values on the right side of [7] is the presence of a metal ion in  $\langle V_{ionic} \rangle$ . In the equation above,  $\langle V_{sol} \rangle$  represents the potential

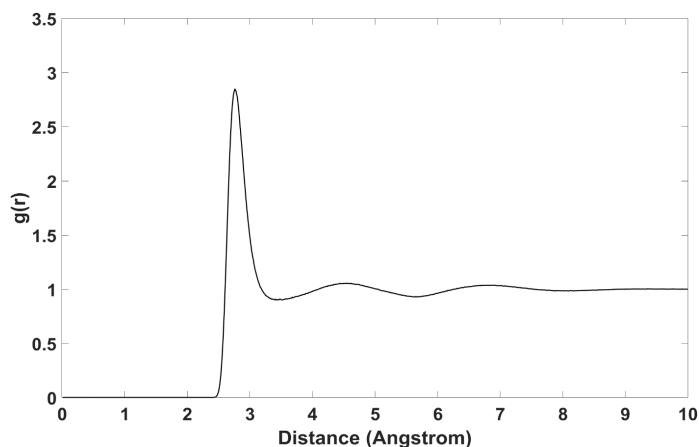


**Figure 1.** Radial distribution function for a system of pure water (500 water,  $r_c = 10$  Å,  $\alpha = 0.32$  Å<sup>-1</sup>). This indicates the probability of finding relative oxygen-oxygen distances within the water system.

energy of ion solvation,  $\langle V_{ionic} \rangle$  represents the potential energy of the ionic system, and  $\langle V_{water} \rangle$  represents the potential energy of pure water, each of which is calculated using [1] with potential [4].

During the simulations, metal to oxygen radial distribution functions were also produced to observe the structure of the system. Radial distribution functions (represented as  $g(r)$  in this work) give structural information by showing probable distances between particles relative to a completely random ideal gas. Maxima thus represent repeated/likely distances within a simulation, where values near 1 indicate a lack of order. Coordination numbers can also be calculated from  $g(r)$  via

$$N_c = 4\pi\rho \int_a^b g(r)r^2 dr, \quad [8]$$

where  $N_c$  is the coordination number, and  $\rho$  is the number density of the system.<sup>14</sup> In this work the coordination number for each metal ion was thus calculated by choosing limits  $a$  and  $b$  to capture the first coordination peak in the radial distribution function.

## Results and Discussion

The process described above was first applied and optimized for a system of pure water. A cutoff radius was chosen, and accurate total potential energies (relative to previous simulations<sup>15</sup>) were produced through parameterization of  $\alpha$ . To confirm structural integrity, the radial distribution function for water (Figure 1) was analyzed and shown to match literature forms as well, with similar first and second peak locations and magnitudes (Table 3).<sup>11</sup>

A separate parameterization of  $\alpha$  was undertaken for metal systems as the net charge of the system was no longer neutral. It was found that an  $\alpha$  of 0.22 Å<sup>-1</sup> yielded the best results for all three ionic systems. The Pb<sup>2+</sup> (aq) simulation yielded the closest solvation energy to accepted values with only a 2.14% difference, while

**Table 3.** Water Radial Distribution Function Peak Locations and Coordination Numbers versus Literature Values

System	Coordination Number	1st Peak Position (Å)	1st Peak Maximum	2nd Peak Position (Å)	2nd Peak Maximum
H <sub>2</sub> O	5.2	2.76	2.85	4.55	1.05
Lit. H <sub>2</sub> O <sup>3</sup>	4.7	2.87	3.09	4.48	1.14

<sup>1</sup>Literature solvation energy was from a 6 water cluster and not a fully aqueous system

**Table 4.** Calculated Solvation Energies of Aqueous Systems versus Literature Results.

System	Potential Energy (kcal/mol)	Solvation Energy (kcal/mol)	Literature Solvation Energy (kcal/mol) <sup>14,15</sup>	% Difference
H <sub>2</sub> O	-4947.7	-	-	-
Zn <sup>2+</sup> (aq)	-5465.9	-518.2	-	-
Cd <sup>2+</sup> (aq)	-5451.8	-507.0	-436.9	14.86%
Pb <sup>2+</sup> (aq)	-5314.4	-366.8	-359.0	2.15%

**Table 5.** Peak Locations Magnitudes, and First Shell Coordination Numbers for Metal-Oxygen Radial Distribution Functions versus Literature Values

System	Coordination Number	1st Peak Position (Å)	1st Peak Maximum	2nd Peak Position (Å)	2nd Peak Maximum
Zn <sup>2+</sup> (aq)	4.0	1.62	36.90	3.02	2.18
Lit. Zn <sup>2+</sup> (aq) <sup>1</sup>	6.0	2.12	19.10	4.10	1.95
Cd <sup>2+</sup> (aq)	4.0	1.65	33.88	3.02	1.90
Lit. Cd <sup>2+</sup> (aq) <sup>3</sup>	6.0	2.08	23.75	4.24	2.10
Pb <sup>2+</sup> (aq)	9.0	2.54	14.48	4.70	2.23
Lit. Pb <sup>2+</sup> (aq) <sup>3</sup>	6.0	2.56	12.96	4.79	1.95

Zn<sup>2+</sup> (aq) and Cd<sup>2+</sup> (aq) simulations yielded solvation energies that differed more significantly from literature (Table 4). Please note, the only experimental solvation energy for Zn<sup>2+</sup> was not available therefore no literature comparison could be made.<sup>17</sup>

In an analysis of the radial distribution function results for the hydrated ion systems, our simulation for Pb<sup>2+</sup> (aq) again matched well with those found using MD methods in terms of peak positions and heights.<sup>3</sup> However, the radial distribution functions of Zn<sup>2+</sup> (aq) and Cd<sup>2+</sup> (aq) did not match previous work and showed a first peak position that was far too close to the ion (Figure 2).<sup>1,3</sup> Radial distribution functions were used to calculate coordination numbers via equation [8], resulting in coordination numbers that were too low relative to established procedures (Table 5). All three metals were found to have 6 waters within their first coordination sphere with octahedral geometries in literature (Table 5).<sup>1,3</sup> Our results indicate coordination numbers that were lower than those in the literature for Zn<sup>2+</sup> and Cd<sup>2+</sup> systems, while the coordination number for Pb<sup>2+</sup> was found to be 9.0 (which is higher than expected). While Pb<sup>2+</sup> was found to have a higher first sphere coordination numbers in some studies,<sup>16</sup> the simulation resulting in tetrahedral geometries for Cd<sup>2+</sup> and Zn<sup>2+</sup> indicates incomplete accounting of interactions. This may suggest that the terms shown in [5] and [6] cannot be neglected for ionic systems.

## Conclusions

Utilizing Wolf's method in conjunction with a Monte Carlo integration technique proved to provide a computationally efficient process that could accurately reproduce the energetics and structural information for a system of pure water and aqueous Pb<sup>2+</sup> (aq). The validity of Wolf's method for homogeneous systems has been previously established,<sup>5-8</sup> however during this study the energetic and structural results for heterogeneous aqueous systems provided mixed results. The solvation energy and radial distribution function for Pb<sup>2+</sup> (aq) matched established literature values, but Zn<sup>2+</sup> (aq) and Cd<sup>2+</sup> (aq) simulations led to solvation energies that were too negative and metal to oxygen distances that were shorter than those found in previous work.<sup>1,3,16-17</sup> While the version of Wolf's method that was utilized provided a computationally efficient way to deal with long range electrostatic interactions, the inconsistent

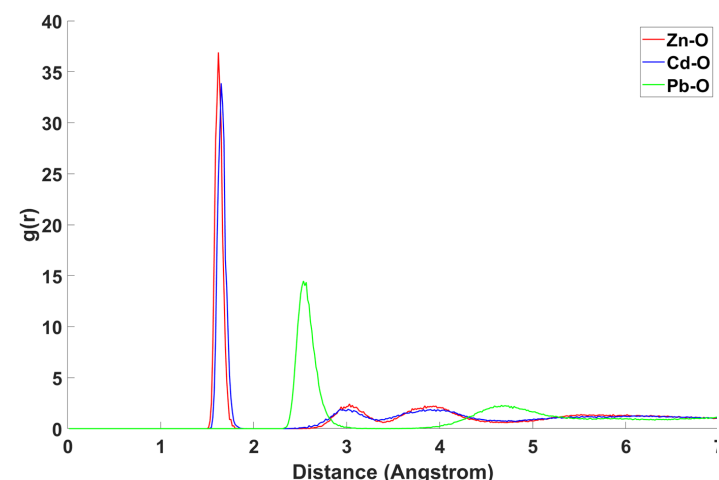


**Figure 2.** Radial distribution functions for Zn-O (red), Cd-O (blue) and Pb-O (green). The first and second peaks for each function infer the first and second coordination sphere positions.

results prompt an analysis of all aspects of the simulation. Deviations could have been caused in part by the neglect of the aforementioned long ranged and self-terms ([5] and [6]).<sup>6,8</sup> While it was determined that these terms had approximately zero contribution to the energetics of a homogenous system, it is possible that the introduction of higher charges (in the form of the divalent cations) makes the long range or self-terms significant and thus non-negligible. In a recent study by Rahbari et al., the DSF form of Wolf's method was utilized in order to evaluate potential interactions within a heterogeneous mixture of water and ethanol.<sup>19</sup> While this was not a charged system, additional modifications were required to accurately evaluate the mixture.<sup>19</sup>

Future work will be aimed at continuing to address the validity of the usage of Wolf's Method within aqueous systems. Simulations could be carried out with [5] and [6] included in the calculation of total potential energy. Additionally, the use of a Lennard-Jones 12-6 potential has been suggested to be inadequate for highly charged systems.<sup>20</sup> To possibly produce more accurate interactions, potential functions such as the Lennard-Jones 12-6-4 could be adopted.<sup>20</sup> Further, the rigidity of water in our simulations could be lifted, as it has been indicated that a flexible water molecule may be better for modeling solvation of ions.<sup>21</sup> If successful, other aqueous systems could be studied again with the goal of providing computational efficiency with minimal complexity, and thus allowing for such interesting and relevant work to be carried out in an undergraduate setting.

## Acknowledgements

We would like to thank Dr. James A. Beres and Merry Jean Beres and the Shippensburg University Undergraduate Research Program for funding this project, and the Shippensburg Chemistry Department for the use of their facilities.

## References

- 1) Stote, R. H.; Karplus, M. *Proteins*, **1995**, 23, 12–31.
- 2) Fu, F.; Wang, Q. *J. Environ. Manage.*, **2011**, 92, 407–418.
- 3) de Araujo, A. S.; Sonoda, M. T.; Piro, O. E.; Castellano, E. E. *J. Phys. Chem. B*, **2007**, 111 (9), 2219–2224.
- 4) Hoyer, C. E.; Kegerreis, J. S. *J. Chem. Educ.*, **2013**, 90, 1186–1190.
- 5) Fennell, C. J.; Gezelter, J. D. *J. Chem. Phys.*, **2006**, 124, 234104.
- 6) Fanourgakis, G. S. *J. Phys. Chem. B*, **2015**, 119, 1974–1985.
- 7) McCann, B. W.; Acevedo, O. *J. Chem. Theory Comput.*, **2013**, 9, 944–950.
- 8) Waibel, C.; Feinler, M. S.; Gross, J. *J. Chem. Theory Comput.*, **2019**, 15, 572–583.
- 9) Waibel, C.; Gross, J. *J. Chem. Theory Comput.*, **2018**, 14, 2198–2206.
- 10) Yonezawa, Y.; Fukuda, I.; Kamiya, N.; Shimoyama, H.; Nakamura, H. Free Energy *J. Chem. Theory Comput.*, **2011**, 7, 1484–1493.
- 11) Mark, P.; Nilsson, L. *J. Phys. Chem. A*, **2001**, 105, 9954–9960.
- 12) Dezfoli, A. A.; Mehrabian, M. A.; Hashemipour, H. *Chem. Eng. Commun.*, **2015**, 202, 1685–1692.
- 13) Inada, Y.; Mohammed, A. M.; Loeffler, H. H.; Rode, B. M. *J. Phys. Chem. A*, **2002**, 106, 6783–6791.
- 14) Park, S.-H.; Sposito, G. *J. Phys. Chem. B*, **2000**, 104, 4642–4648.
- 15) Berendsen, H. J. C.; Grigera, J. R.; Straatsma, T. P. *J. Phys. Chem.*, **1987**, 91, 6269–6271.
- 16) Johnson, K. J.; Cygan, R. T.; Fein, J. B. *Geochim. Cosmochim. Acta*, **2006**, 70, 5075–5088.
- 17) Parchment, O. G.; Vincent, M. A.; Hillier, I. H. *J. Phys. Chem.*, **1996**, 100, 9689–9693.
- 18) León-Pimentel, C. I.; Martínez-Jiménez, M.; Saint-Martin, H. *J. Phys. Chem. B*, **2019**, 123, 9155–9166.
- 19) Rahbari, A.; Hens, R.; Jamali, S. H.; Ramdin, M.; Dubbeldam, D.; Vlugt, T. J. H. *Mol. Simul.* **2019**, 45, 336–350.
- 20) Li, P.; Song, L. F.; Merz, K. M. *J. Phys. Chem. B*, **2015**, 119, 883–895.
- 21) Yuet, P. K.; Blankschtein, D. *J. Phys. Chem. B* **2010**, 114 (43), 13786–13795.